# Non-Chaotic Strange Attractors from the Quasi-Periodically driven Duffing Oscillator

Hitesh Kumar*
Project Supervisor: Dr. Philip Ramsden
Department of Mathematics
Imperial College London
United Kingdom

October 19, 2017

**Abstract**

The focus of this investigation is to perform qualitative analysis on the attractors that arise from the quasi-periodically driven Duffing oscillator. In this report we examine some methods that can be used to determine non-chaotic strangeness. We then discuss their reliability and performance, and the meaning of their results to determine the most suitable ones for such an investigation. Finally, these methods are applied and we show the existence of strange non-chaotic attractors (SNA's) in the quasi-periodically driven Duffing oscillator.

*Funding for this project provided by the EPSRC (Engineering and Physical Sciences Research Council)

# Contents

**1 The Duffing oscillator** **3**

**2 Numerical Solutions and Attractors** **3**
2.1 Numerical solutions and chaotic behavior . . . . . 3
2.2 Poincaré sections and Attractors . . . . . 4
2.3 Introducing Quasi-periodic driving . . . . . 5

**3 Methods for quantitatively determining chaos** **7**
3.1 chaotic vs. non-chaotic behavior . . . . . 7
3.1.1 The Fourier transform . . . . . 7
3.1.2 Lyapunov exponents . . . . . 9
3.1.3 The Zero-One test . . . . . 10
3.2 Measuring the geometric strangeness of attractors . . . . . 11
3.2.1 Lyapunov dimension . . . . . 11
3.2.2 Correlation dimension . . . . . 12
3.2.3 Box/Sphere counting dimension . . . . . 13

**4 Discovering Non-Chaotic Strange Attractors** **14**
4.1 Process of finding SNA's . . . . . 14
4.1.1 Method . . . . . 14
4.1.2 Performance . . . . . 15
4.2 Results . . . . . 16

**A MATLAB Code** **18**

# 1 The Duffing oscillator

First studied in depth by Georg Duffing [1], the Duffing equation arises from observing what the motion of a system slightly more complex than the damped simple harmonic oscillator might look like. For example, if a spring that does not exactly obey Hooke's law undergoes forcing and damping, then the equation commonly used for such a system no longer accurately describes the motion. We introduce the simplest term which retains the symmetry of the displacement, and so the equation to model such a system becomes:

$$\ddot{x} - \alpha\dot{x} - \beta x - \delta x^3 = \gamma\cos(\omega t) \tag{1}$$

Depending on the value of $\delta$, the behavior of this system is now vastly different to what is observed in the simple harmonic case. Most notably, for some parameter values, the sensitivity to initial conditions is extremely high, and orbits separated in space by a small amount will diverge exponentially with time.

Despite the lack of an analytic solution, we can still observe the solutions to this. With a substitution, we can model the equation with the 3-Dimensional system of two ODE's:

$$\begin{aligned} y &= \dot{x} \\ \dot{y} &= \alpha y + \beta x + \delta x^3 + \gamma\cos(\omega t) \end{aligned}$$

(Note that W.L.O.G, we can set $\omega = 1$, as we could observe the behavior of the system for any other value of $\omega$ by scaling the other parameters). Here our 3 dimensions are position ($x$), speed ($\dot{x}$) and time ($t$). Now if we integrate this system we can obtain $x$ and $\dot{x}$ and observe its behavior as $t$ changes.

# 2 Numerical Solutions and Attractors

## 2.1 Numerical solutions and chaotic behavior

The method of choice for both accuracy and performance is Runge-Kutta $4^{th}$ order numerical integration, the implementation of which can be found in the appendix. Using MATLAB, we can now observe the solutions to the system, subject to initial conditions $x(0) = 1$ and $\dot{x} = 0$ (these will be the standard initial conditions used throughout the project unless stated otherwise in later sections).

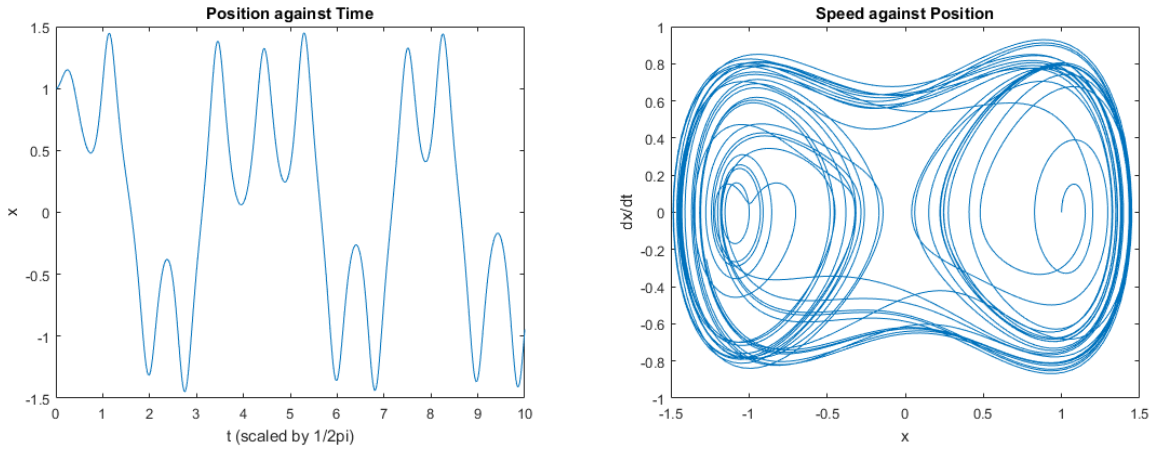


Figure 1: Position against time (left), t has been scaled by a factor pf $\frac{1}{2\pi}$ for clarity. Speed against Position (right), for $60\pi \leq t \leq 100\pi$

For the parameters $\alpha = -0.2$, $\beta = 1$, $\delta = -1$, $\gamma = 0.3$ and $\omega = 1$, we observe what is seemingly aperiodic behavior, producing geometrically complex graphs. If the non-linear stiffness constant $\delta$ is decreased to -3 for example, and if we skip the initial iterations to let the effects of the initial conditions dissipate, we will observe what seems to be periodic behavior. To observe the sensitivity to initial conditions, we simply plot solutions for initial conditions varying by a relatively small amount ($10^{-4}$):

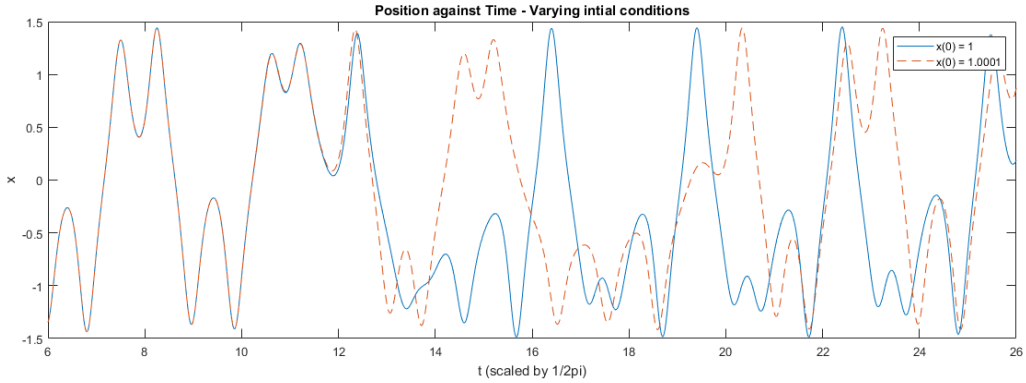


Figure 2: By changing the initial position by such a small amount, the displacement at any given time after some point ($\approx 11.5\pi$ in this case) can no longer be approximated to any reasonable degree of accuracy from the previous solution.

Figure 3 shows how the oscillator displays sensitive dependence on initial conditions, causing unpredictable changes to the dynamics. Hence (arguably) the simplest method to qualitatively determine chaotic behavior is by observing the geometric complexity of the Poincaré section formed.

## 2.2 Poincaré sections and Attractors

A Poincaré section of an $n$-dimensional flow is essentially the set of points obtained by taking the value of $n-1$ dimensions whenever the one chosen dimension takes certain values[2]. This allows us to generate the set of points that a typical orbit (orbits of the long term solution, after sufficiently many iterations have passed) tends towards

in $n-1$ dimensional space, for a large range of initial conditions. (when the limit to infinity of the iterations is taken, this set is called an attractor, but we will refer to our "approximations" as attractors in this paper for simplicity). For our system, we record the values taken by the position and speed dimensions whenever our time dimension take the value of some multiple of $2\pi$.

For a chaotic system, the attractor will be geometrically complex, or "strange"[3] and will have distinct values for many other of its quantifiable properties discussed in later sections. One would think therefore that non-chaotic attractors should always be geometrically simple and hence non-strange, but as we will observe, this is not true. Strange, non-chaotic attractors (SNA's) arise when the system is not sensitive to the same small changes in initial conditions, but yet the attractors produced display geometric strangeness. It is determining whether or not the attractors are strange (or even how strange) that is the issue.

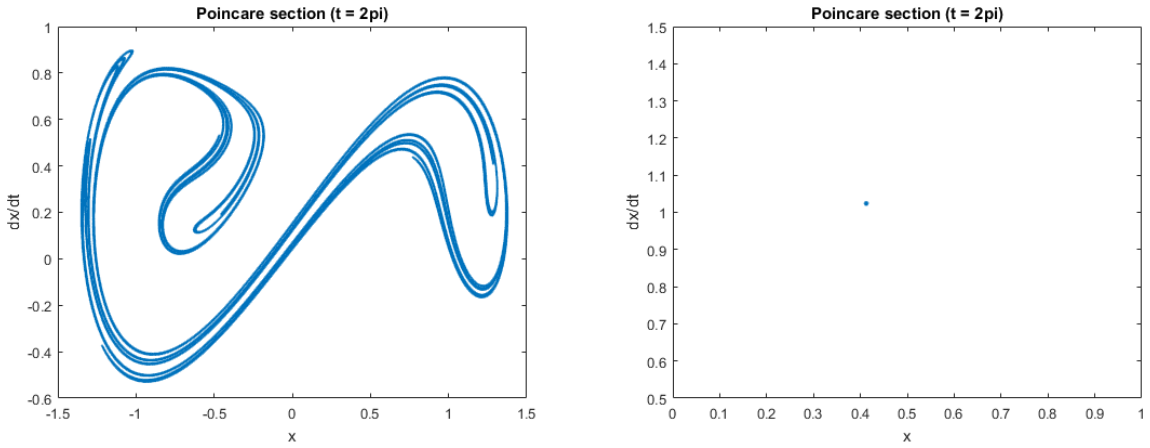


Figure 3: Attractors for the same parameters described above, with the exception of $\delta = -1$ in the chaotic case (left) and $\delta = -1.65$ in the non-chaotic case (right)

## 2.3 Introducing Quasi-periodic driving

To study the more complex and less well understood behavior occurring under quasi-periodic driving, we introduce an additional term to the driving force, giving the system:

$$\begin{aligned} y &= \dot{x} \\ \dot{y} &= \alpha y + \beta x + \delta x^3 + \gamma_1 \cos(\omega_1 t) + \gamma_2 \cos(\omega_2 t) \end{aligned}$$

Note that if $\frac{\omega_2}{\omega_1} \in \mathbb{Q}$, then we simply have periodic driving, hence we require the ratio to be irrational. As any representation of an irrational number on a computer cannot have infinite precision, we must work around the issue by 1) taking advantage of the periodicity of the cosine function, and 2) using values for $\omega_1$ and $\omega_2$ such that $\frac{\omega_2}{\omega_1}$ is as "difficult" as possible to be approximated by a computer.

We can Achieve 2) by setting $\omega_1 = 1$ and using the reciprocal of the 'Golden ratio',

$\phi = \frac{\sqrt{5}-1}{2}$ for $\omega_2$. This particular value is the "most" irrational number in the sense that it takes the greatest number of decimal points to approximate to the same precision as it would for other irrational values[4] (To see this quite easily, simply observe how the denominators in the continued fraction form for this number compare to denominators in other irrational numbers such as $\pi$). To achieve 1), we might think to set $t = 0$ once it reaches $2\pi$, however if we do so, we find the amplitude of the force varies incorrectly as $t$ is re-set to 0 before $\omega_2 t = 2\pi$.

Instead, for the second component of the driving force only, we scale time by $\phi$, effectively using another variable (or dimension) which we label $\tau$, which can be reset independently of $t$. This now allows us to correctly vary the driving force with time. Our system now becomes:

$$\begin{aligned} y &= \dot{x} \\ \dot{y} &= \alpha y + \beta x + \delta x^3 + \gamma_1 \cos(t) + \gamma_2 \cos(\tau) \end{aligned}$$

Where we have $\tau_{n+1} = \tau_n + 2\pi \mod 2\pi$. Hence where before we had the map:

$$(x_{n+1}, \dot{x}_{n+1}) = \Phi_1(x_n, \dot{x}_n) \qquad (\mathbb{R}^2 \to \mathbb{R}^2)$$

we now have the map:

$$(\tau_{n+1}, x_{n+1}, \dot{x}_{n+1}) = \Phi_1(\tau_n, x_n, \dot{x}_n) \qquad (\mathbb{R}^3 \to \mathbb{R}^3)$$

As a consequence of introducing a new dimension, we now have in essence, a 4-dimensional dynamical system which we can generate a 3-dimensional attractor (where $0 \leq \tau \leq 2\pi$).

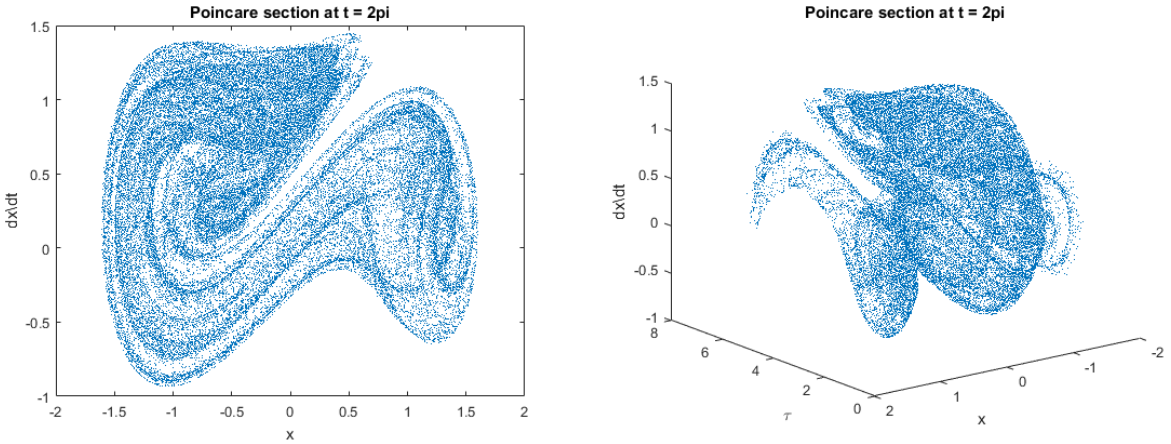


Figure 4: for $\alpha = -0.2$, $\beta = 1$, $\delta = -1$, $\gamma_1 = 0.3$ and $\gamma_2 = 0.3$, we see the 2-dimensional attractor (left) exhibiting geometric strangeness as expected, however the 3-dimensional attractor gives a much richer view of the dynamics.

# 3 Methods for quantitatively determining chaos

Finding a non-chaotic strange attractor is not necessarily a matter of luck. One can start with a periodically driven non-chaotic system and increase the amplitude of the component of the force with the irrational frequency, with the hope that the system will remain non-chaotic whilst the attractor becomes strange. Below are some algorithms that were implemented and tested in this investigation to give some value quantitative measurement of how chaotic the systems are as we change the parameters.

One of the test cases we used to determine the reliability of these methods was a "candidate" SNA, suspected to to be one due to not displaying the sensitivity to initial conditions which would be expected if it corresponded to a chaotic system.

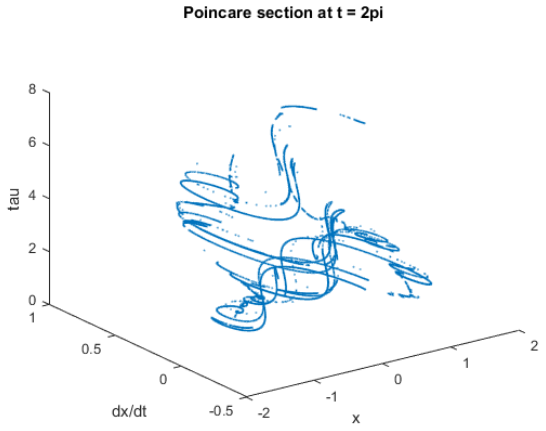


Figure 5: for $\alpha = -1$, $\beta = 1$, $\delta = -1$, $\gamma_1 = 0.3$ and $\gamma_2 = 0.4782$, a suspected SNA was found after observing the lack of sensitivity to initial conditions. From here on, it was used as a test case to assess the reliability of all the methods we discuss.

## 3.1 chaotic vs. non-chaotic behavior

Initially, it would make sense to quickly and easily plot position against time for various values of the parameters and observe whether or not we see the dynamics change significantly with a small change in initial conditions. However, we come across an issue. Deciding how far in time to look to observe the divergence of the flows. For some parameters, we can only see the flows diverging from each other after thousands of cycles of the driving force, whereas for others, it occurs almost instantly after we begin evolving the system. Additionally, even if we did observe some divergence due to a change in initial conditions, how would we determine that it is significant enough of a change to justify classing the system as chaotic? That is to say, how can we be more precise with the judgment?

### 3.1.1 The Fourier transform

If we take the Fourier transform of the solution, we would be able to find which frequencies are most prominent in the oscillations, giving us an idea of whether the oscillations exhibit periodicity. As we need a discrete transform for our data, we use MATLAB's inbuilt function, FFT[5], and transform the data to represent it as needed.

Upon applying the FFT to data for various parameters, we find that for parameter values that are quite apparently chaotic, the transformed data contains what seems like noise, with small number of observable peaks. For periodic data, we see a few, much clearer peaks.

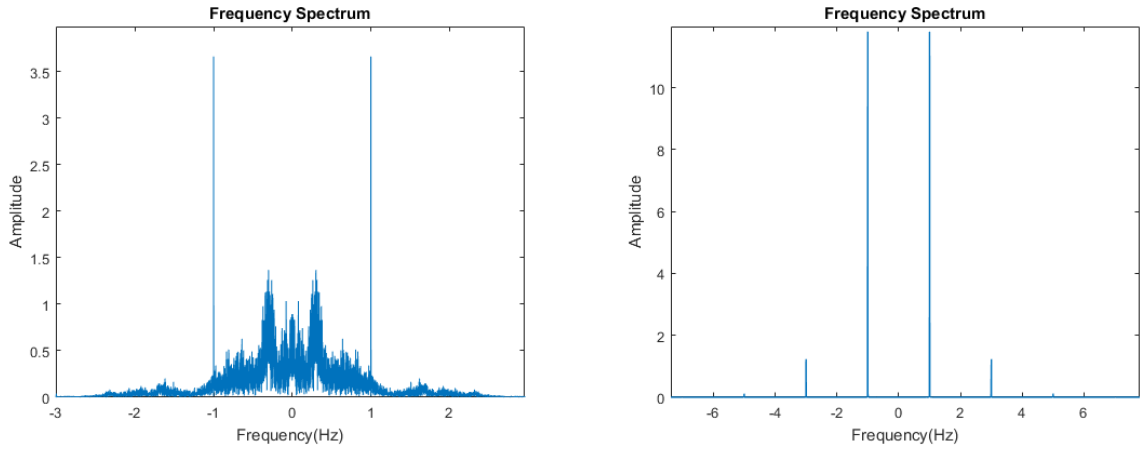


Figure 6: For chaotic parameters, we observe a seemingly noise filled spectrum with one very distinct peak, whereas from the non-chaotic parameters, we see 3 distinct peaks at 1, 3 and 5 Hz.(same parameters as used in figure 3

Additionally we see that for the test SNA, we get interesting results, where the frequency spectrum seems to have multiple distinct peaks whilst also showing a large amount of noise. Interesting results indeed, but this does mean that we cannot rely on the Fourier transform to clearly distinguish between chaotic strange dynamics and the non-chaotic variants.

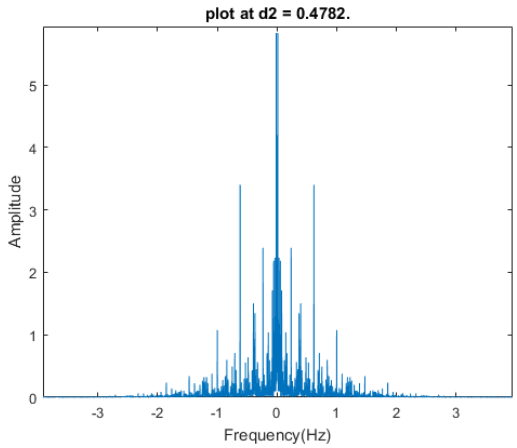


Figure 7: For the test SNA, we observe a large number of distinct peaks, yet it remains unclear where we can draw the line between a significant frequency and noise.

Performance-wise, as an inbuilt function, the FFT not only runs much faster due to it being compiled, but is also numerically stable unlike the current implementation written by us. Though it is very quick, observing the spectrum for each and every attractor we generate will become a time consuming task, and as of yet there seems to be no method to qualitatively analyse the frequency spectrum to derive a usable result.

### 3.1.2 Lyapunov exponents

The Lyapunov exponents are essentially values that represent the rate of separation of nearby orbits for flows in each dimension. The concept arises from the fact that two trajectories with an initial separation distance $d(0)$ in any dimension will diverge at an exponential rate, i.e $d(t) = e^{\lambda t} d(0)$.[6]. Here, $\lambda$ is the Lyapunov exponent.

Finding the largest exponent is a simple task. We run the solution until the short term effects of the initial condition have decayed, (usually $t = 2 \times 10^5 \pi$ is sufficient) and then introduce a small perturbation $d(0)$ in each dimension:

$$\begin{pmatrix} t \\ \tau \\ x \\ \dot{x} \end{pmatrix} \rightarrow \begin{pmatrix} t + d(0) \\ \tau + d(0) \\ x + d(0) \\ \dot{x} + d(0) \end{pmatrix}$$

The Magnitude of $d(0)$ was chosen to be $10^{-4}$, 4 orders of magnitude smaller than most of the parameters of the system. We now iterate both the unperturbed system, and the newly perturbed system once, and calculate the magnitude of separation between them, $d(t)$. We then calculate $\frac{1}{t} \log(\frac{d(t)}{d(0)})$ in order to extract a measurement of $\lambda$, $\lambda_i$ and add it to a running sum, which after all iterations is averaged to give an estimate:

$$\lambda = \frac{1}{N} \sum_{i=1}^{N} \lambda_i$$

.
However, we must keep in mind that if we do not re-scale the separation back to its original size after each calculation and the system happens to be chaotic, we may observe the flow undergo folding and the orbits will converge or even intersect temporarily, giving an inaccurate estimate of $\lambda$.

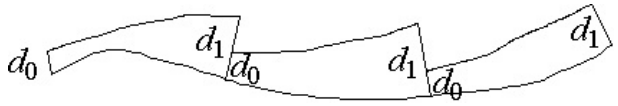


Figure 8: In this example[8], we can infer why it is necessary to rescale the error back down to prevent folding and hence inaccurate results.

Of course, in reality the true value of the exponent is obtained by taking the limit of the above as $N \rightarrow \infty$, however in practice we observe the value converging to three decimal places after around $10^6$ iterations. Naturally, the exponents for $t$ and $\tau$ should be 0, as there is no divergence or convergence occurring in these dimensions. However, what we find is that we only get one value repeated four times and that is the value of the largest exponent.

This is caused by the most chaotic dimension (or the least non-chaotic dimension) interfering with the direction of the separation and hence "pulling" the separation in all dimensions to the same direction. We deal with this by iterating four versions of the same system simultaneously:

$$\begin{pmatrix} t \\ \tau \\ x \\ \dot{x} \end{pmatrix} \to \begin{pmatrix} t + d(0) \\ \tau \\ x \\ \dot{x} \end{pmatrix}, \begin{pmatrix} t \\ \tau + d(0) \\ x \\ \dot{x} \end{pmatrix}, \begin{pmatrix} t \\ \tau \\ x + d(0) \\ \dot{x} \end{pmatrix}, \begin{pmatrix} t \\ \tau \\ x \\ \dot{x} + d(0) \end{pmatrix}$$

Now after each iteration, we calculate the separation as usual and add this value to the running sum, but additionally we now ortho-normalise the separations to both rescale them and to prevent the "pulling" effect of the least non-chaotic dimension. This is achieved by applying a variation of the Gram-Schmidt algorithm we developed.(The exact process of finding each exponent in our case can only be summarised in this report, but a detailed explanation can be found in [7]).

| Parameters | Exponents ($t$, $x$, $\ddot{x}$) |
|---|---|
| (-0.2, 1, -1, 0.3, 0.3) - chaotic | 0, 0.0668,-0.2668 |
| (-0.2, 1, -1.8, 0.3, 0.05) - non-chaotic | 0, -0.1000, -0.1000 |
| (-1, 1, -1, 0.3, 0.4782) - Candidate SNA | 0, -0.1204, -0.8796 |

Table 1: (parameters defined as: $(\alpha, \beta, \delta, \gamma_1, \gamma_2)$). The lyapunov exponents show a clear distinction between the chaotic and non-chaotic cases, with the position dimension being the only one that displays chaotic dynamics. The Lyapunov exponents can be considered reliable so long as the values are sufficiently far from zero. $(0.001 > \lambda > -0.001)$

We can be confident that the sign of the position exponent will indicate chaotic against non-chaotic behavior, as it is calculated from the solutions themselves rather than the attractor sets, so there is no scope for this method detecting strange vs non-strange behavior instead. As for speed, the majority of the algorithm is the same as for calculating the solution, and the additions of storing the error, calculating its logarithm and performing ortho-normalisation with rescaling do not significantly affect the running time.

### 3.1.3 The Zero-One test

The Zero-One test developed by G.A.Gottwald and I.Melbourne[9] takes as its input a time series of the data being evaluated and returns, a value between (or close to, in practice) 0 and 1, giving a qualitative method to compare the chaotic behavior of various systems with no information other than their time series. The time series we test is that of the position values of the attractors, as the calculations for the Lyapunov exponents of our systems give very strong evidence that the speed dimension is generally non-chaotic. If we compare results for chaotic parameter values with non-chaotic parameter values, we see the following:

| Parameters | Result |
|---|---|
| (-0.2, 1, -1, 0.3, 0.3) - chaotic | 0.9958 |
| (-0.2, 1, -1.8, 0.3, 0.05) - non-chaotic | -0.0127 |
| (-1, 1, -1, 0.3, 0.4782) - Candidate SNA | 0.9622 |

Table 2: We see that the Zero-One test can determine between strange behavior and non-strange behavior, but not between chaotic and non-chaotic behavior.

Despite the test being very fast and reliable, it did not seem to be able to test what was needed. The Zero-one test under normal circumstances would distinguish chaotic from non-chaotic behavior, however for the SNA test cases we had, it appears to be unable to distinguish between strange and non-strange behavior, making it unreliable to detect SNA's. For this reason, we did not pursue the use of this method any further.

## 3.2 Measuring the geometric strangeness of attractors

For this analysis, we focus on determining the various types of fractal dimension of the attractors themselves to determine their strangeness. We are able to calculate such a value due to the fact that strange attractors demonstrate fractal behavior and so will have non-integer dimension. There are many measures of these dimensions and each of the three we used can be interpreted in different ways which we briefly describe below, However all are based on the same underlying idea of calculating the Renyi Dimension (also known as the "generalised dimension"), $D_q$ for varying values of $q$:[11]:

$$D_q = \lim_{\epsilon \to 0} \frac{1}{1-q} \frac{\ln(\sum_j (L(c_j))^q)}{\ln(\frac{1}{\epsilon})}$$

Where $L$ is the natural measure function, best described by Edward Ott in [11], $c_j$ is the $j^{th}$ "cube" with side length $\epsilon$. In particular for $q = 0, 1, 2$, we have the Box-counting dimension $D_B$, Information dimension $D_I$ and Correlation dimension $D_C$ respectively. Now firstly, we rely on the Kaplan-Yorke conjecture, $D_1 = D_I = D_L$ (where $D_L$ is the Lyapunov dimension described later) to be true. Secondly, we note an important property of the Renyi dimension:

$$q_2 > q_1 \Rightarrow D_{q_2} \leq D_{q_1}$$

These two statements, in our case, mean that if our values for the measures of dimension satisfy $D_C \leq D_L \leq D_B$ then we can be confident that both our implementations work and that our results are reliable.

### 3.2.1 Lyapunov dimension

The Lyapunov dimension, or Kaplan-Yorke dimension[10] (named after J. Kaplan and J. Yorke) is a measure of the fractal dimension calculated from the Lyapunov exponents themselves. This is achieved by first sorting the $n$ Lyapunov exponents in descending order, so that $\lambda_1 \geq \cdots \geq \lambda_n$ and calculating the dimension $D_L$ as:

$$D_L = j + \frac{\sum_{i=1}^{j} \lambda_n}{|\lambda_{n+1}|}$$

Where $j$ is largest integer such that:

$$\sum_{i=1}^{j} \lambda_n \geq 0$$

As with the Lyapunov exponents, we do not include the exponent from the $t$ dimension

in these calculations, hence in our implementation we only have 3 exponents.

For chaotic parameters we will always get one positive exponent from the position dimension, hence a quick calculation by hand would show that $D_L \geq 2$. However, for the case where both non-zero exponents are negative, clearly $D_L = 1$. Its this extremely clear distinction that allows us to so easily tell apart a non-chaotic strange attractor from a chaotic one.

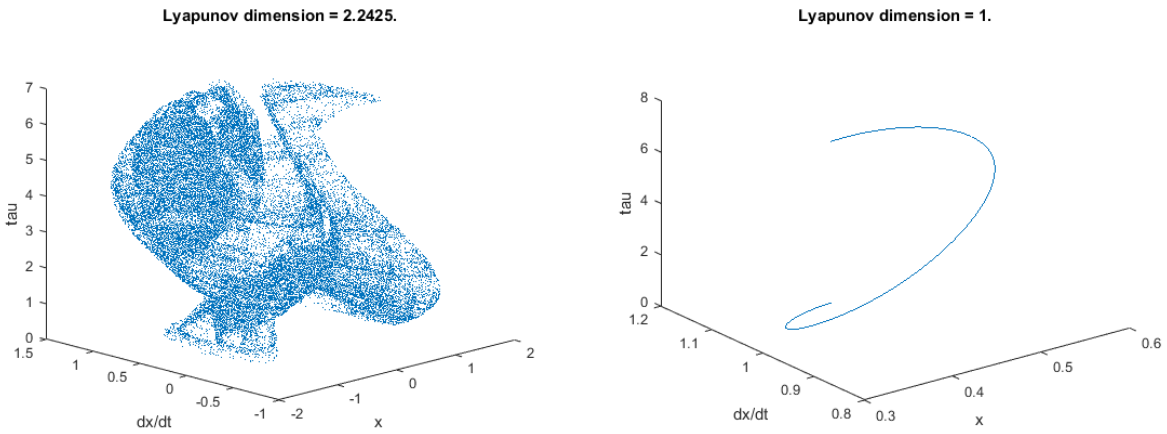


Figure 9: In these cases, the visual distinction is clear, with the chaotic strange attractor having $D_L = 2.24$ and the non-strange attractor having $D_L = 1$.

As for performance, the calculations required after obtaining the Lyapunov exponents are trivial, and so only the accuracy to which we want to determine the exponents affects the time taken to run. As previously found, we get sufficiently accurate values with only $2 \times 10^6$ iterations and so the performance was not an issue.

### 3.2.2 Correlation dimension

Another measure of fractal dimension, which is arguably better suited to finite sets such as subsets of the attractors we generate, is the Correlation dimension. This method relies on the approximation of the correlation sum $C(r)$:

$$C(r) = \lim_{N\to\infty} \frac{1}{N(N-1)} \sum_{i=1}^{N} \sum_{j=i+1}^{N} H(r - |x_i - x_j|)$$

where H is the Heaviside step function, $x$ are the elements of the attractor set and $r$ is the maximum distance between elements we evaluate the Heaviside step function for. This is the probability that two points $x_i$ and $x_j$ are within $r$ distance of each other. For strange attractors, we expect a lower density of points in space giving a significantly higher value for the Correlation dimension than we would expect from a non-strange attractor.

An issue we face is that we cannot take the limit as the number of points tends to infinity. We solve this by instead observing how the Correlation sum changes as we change the distance considered, $r$. If $C(r) \sim r^{D_C}$ then we can plot the logarithms

of the values obtained against the logarithms of the distances and extract $D_C$ as the gradient, through Linear regression.

| Parameters | Correlation dimension |
|---|---|
| (-0.2, 1, -1, 0.3, 0.3)- chaotic | 1.8074 |
| (-0.2, 1, -1.8, 0.3, 0.05) - non-chaotic | 1.0030 |
| (-1, 1, -1, 0.3, 0.4782) - Candidate SNA | 0.8950 |

Table 3: (For the parameter vectors defined as: $(\alpha, \beta, \delta, \gamma_1, \gamma_2)$). the Correlation dimension returns results similar to what we would expect for the test attractors. It is however a surprise to see the unusually low value of $D_c$ for the candidate SNA.

For all of our test attractors, our implementation returns sensible results, showing yet again a very clear distinction between chaotic strange attractors and their non-chaotic counterparts, making this yet another reliable method to obtain a value for the fractal dimension. Somewhat of a surprise is the fact that we get a lower value for the dimension of the SNA than we do for the clearly non-chaotic attractor, a result which we will explore in later sections.

In terms of performance, the double summation in the correlation integral results in a time complexity of $O(N^2)$ ($O(\frac{N^2}{2})$ more specifically), and as we have to re-calculate for multiple values of $r$ to obtain the dimension we get a time complexity of $O(N_r N^2)$ for the algorithm itself. Clearly, even with a what could be considered a minimal 10 values of $r$ and $10^4$ points in the attractor, this already amounts to a number on the order of $10^9$ repetitions of the Heaviside step function, a lengthy task even for high-end machines.

### 3.2.3 Box/Sphere counting dimension

The box counting dimension is yet another way of determining the fractal dimension of a set based on estimating the capacity dimension of an object. The concept behind it is to observe the minimum number of boxes required such that the union of all boxes contains the object, and to see how this number changes as the sizes of the boxes change. Again as with the Correlation dimension, it is assumed that the relationship follows a power law with the power being the Box counting dimension, which can be found through linear regression on the log-log plots.

The implementation used took advantage of the fact that we were processing finite sets. The concept was to translate the attractor so that all points have positive values, and then to round down each point to the nearest integer values below in each dimension. These were then scaled in each dimension by the box size to effectively separate them into the boxes. Finally, determining how many boxes contained at least one point was simply a matter of determining the number of unique points.

| Parameters | Box Counting dimension |
|---|---|
| (-0.2, 1, -1, 0.3, 0.3)- chaotic | 2.3200 |
| (-0.2, 1, -1.8, 0.3, 0.05) - non-chaotic | 1.0169 |
| (-1, 1, -1, 0.3, 0.4782) - Candidate SNA | 1.6812 |

Table 4: The Box count dimension returns sensible results on the first test, and indicated that the Candidate SNA may have a significantly different value

The first implementation relied on a similar method to the Correlation dimension, where each point not already covered by a sphere would be covered and every other point was determined to be inside the sphere or not. Clearly, as this required looking at each of the $N$ points $N-1$ times, we had an algorithm that had a time complexity of $O(N^2)$ at the very least. If the data was pre-processed into boxes, the implementation could have been far more efficient, but regardless the second implementation which runs in linear time would still be faster.

# 4 Discovering Non-Chaotic Strange Attractors

## 4.1 Process of finding SNA's

### 4.1.1 Method

Rather than moving on randomly selected lines in parameter space, we chose to start with a system that was clearly non-chaotic, with $\gamma_2 = 0$. Then we increased $\gamma_2$ in small increments, whilst plotting the attractor for each value, as well as calculating the Lyapunov exponents and the three measures of fractal dimension.

The advantage of this approach as opposed to starting from random parameter values was that we could observe the point at which a non-chaotic non-strange attractor would become strange, and additionally observe the bifurcations and how the values of the Lyapunov exponents and fractal dimensions changed through them.

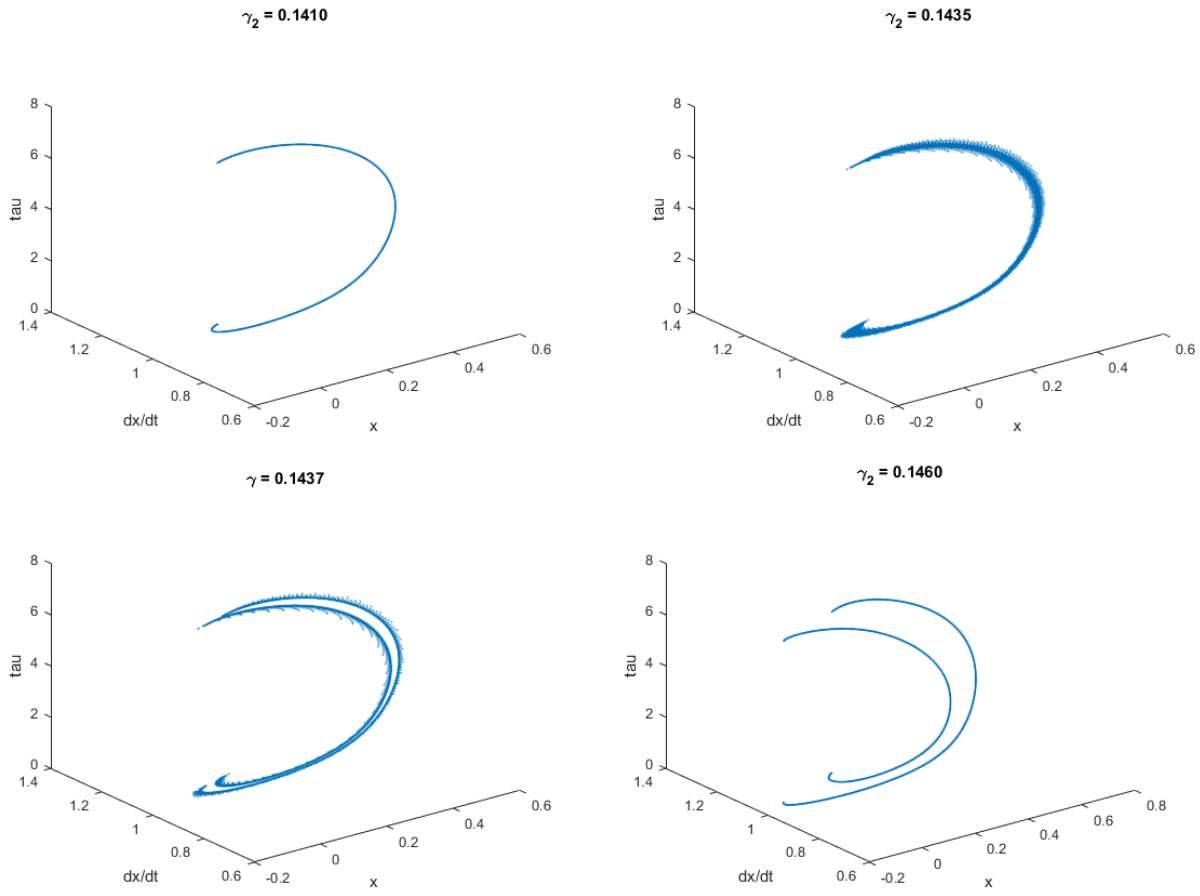


Figure 10: Here we can see a bifurcation occurring as the value of $\gamma_2$ increases from 0.1410 to 0.1460.

As for the choice of methods, we decided to use the sign of the Lyapunov exponents as the indicator of chaotic behavior, and would not consider cases where the exponent was too close to zero. The strangeness of the attractor was determined by observing how all three measures of the fractal dimension changed as $\gamma_2$ increased. This allowed us to initially gain a better understanding of the results from each algorithms, giving us a better idea of what to expect from each measure of fractal dimension as the systems underwent bifurcations. After testing the algorithms, it also made the classification of SNA's much more reliable as we had more than one value that significantly changed to indicate the existence of non-strange attractors.

### 4.1.2 Performance

We found that the 3D plot of the attractor, the calculation of the lyapunov exponents and the Lyapunov dimension would collectively take time approximately equal to 3 seconds to run if the attractor were to contain $10^5$ points, and the exponents were to be calculated with a total of $2 \times 10^5$ iterations of the solution. The calculation of the Box-counting dimension would take time on the order of 10 seconds for an attractor with $10^5$ points. However the Correlation dimension would take approximately $5 \times 10^2$ seconds to run for the same number of points on an attractor, which is clearly not feasible. For this reason, all the initial calculations were done for an attractor with $10^5$

points with the exception of the calculation of the Correlation dimension, which was done for the exact same parameters as the other calculations but only for $10^4$ points. Of course, for suspected SNA's we would confirm our results with more points. Whilst this running time reduction does impact the accuracy of the value for the Correlation dimension, we determined it would still be reliable as the changes in this value expected when a strange attractor transitions into non-strange attractor were significant enough to be noticed.

## 4.2 Results

Having started from the 3-dimensional system that we originally found to be non-chaotic, we discovered the candidate SNA first (which we initially suspected of being such an object due to the lack of sensitivity to initial conditions). After more investigation we found that indeed it was a strange non-chaotic attractor.

In addition to this case, many more were found, at parameters such as:

| Parameters |
|---|
| (-0.2, 1, -1, 0.3, 0.4782) |
| (-0.5, 1.5, -0.8, 0.4, 0.7878) |
| (-0.5, 1.5, -0.8, 0.4, 1.0101) |
| ($\sqrt{7}$, $\sqrt{7}$, $\sqrt{7}$, $\sqrt{7}$, 0.0959) |
| (-0.3, 0.9, -1.5, 0.4, 0.4251) |

Table 5: Some examples of the parameter values we found SNA's to exist in. These values were inside regions in parameter space in which SNA's existed, however these were the strongest cases found in said regions.

Quite surprisingly, we found reasonably strong evidence for a SNA where all the fixed parameters are $\sqrt{7}$.

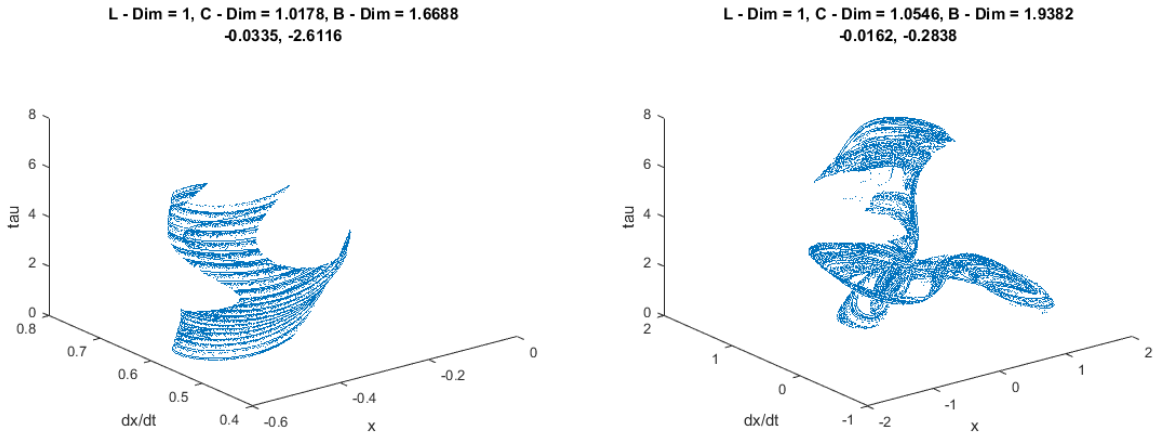


Figure 11: Whilst the lyapunov exponents (last two numbers) for the position dimension are weakly non-chaotic, the values for the Correlation and Box-counting dimensions strongly suggest a SNA in both cases.

Another surprising discovery is that $\sqrt{7}$ in continued fraction form has denominators $(2, \dot{1}, 1, 1, \dot{4})$ with the final 4 digits recurring. This means that it is a reasonably

difficult to approximate irrational to use as a driving frequency. Suspected SNA's were found with the irrational driving frequency being $\sqrt{7}$, but not confirmed or recorded due to time restraints.

Recall the inequality presented earlier as an important result of varying $q$ in the calculation of the Renyi Dimension:

$$D_C \leq D_L \leq D_B$$

One method to determine the reliability of both our algorithms and hence results was to find $D_C$, $D_L$ and $D_B$ all satisfy the inequality given, however at first sight this does not seem to be the case. We find $D_B$ to indeed have the largest value of the three measures of fractal dimension, with the Lyapunov dimension being smaller, however for many non-chaotic attractors, we see that $D_C$ is greater than $D_L$ on the order of $10^{-3}$. This can be observed in the test cases above, where the clearly non-chaotic case gives $D_L = 1$ but $D_C = 1.0030$.

We dismiss this as a a result of the inefficiency of the algorithm to calculate $D_c$, however we sought to justify this. Hence we calculate $D_C$ for attractors generated with the same parameters but for varying numbers of points.

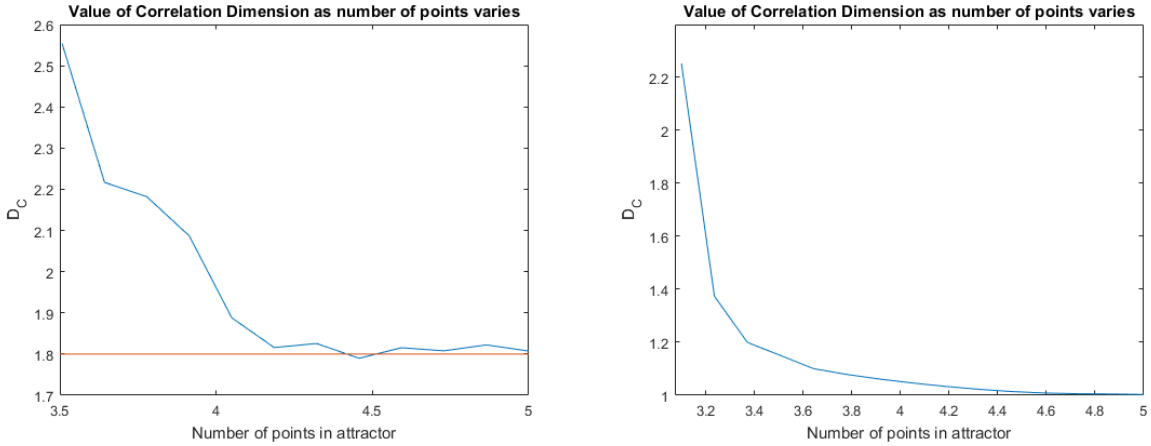


Figure 12: We see that the Correlation dimension decreases as the number of points in an attractor increases. The convergence occurs much quicker for the Chaotic attractor (left), but much more slowly for non-chaotic attractors (right). The x-axis displays the number of points to the log base 10

We see very clearly that as we increase the number of points from $10^3$ to $10^5$, the value of the correlation dimension decreases significantly. Additionally, we see that the values appear to converge much faster for the chaotic attractors than for the non-chaotic non-strange attractors, so we can now assume the true value of the correlation dimension (that is, if the limit as the number of points tend to infinity) for non-chaotic attractors would be 1, satisfying the inequality.

# A MATLAB Code

As all the functions together are far too large to be attached here, All the code used in this project along with a detailed explanation of how it works is available on my GitHub at

`https://github.com/FistOfHit`

# References


[1] Hans Jürgen Korsch, Hans-Jörg Jodl, Timo Hartmann. *Chaos*. Berlin, Springer; 2008. Available from: https://link.springer.com/book/10.1007/978-3-540-74867-0#about [Accessed 04 July 2017]

[2] Weisstein, Eric W. *Surface of Section*. Available from: http://mathworld.wolfram.com/SurfaceofSection.html [Accessed 15 July 2017]

[3] David Ruelle, *What is a strange attractor*. 2006. Available from: http://www.ams.org/notices/200607/what-is-ruelle.pdf [Accessed 04 July 2017]

[4] Weisstein, Eric W. *Golden Ratio*. Available from: http://mathworld.wolfram.com/GoldenRatio.html [Accessed 02 August 2017]

[5] MathWorks. *Fast Fourier Transform*. Available from: https://uk.mathworks.com/help/matlab/ref/fft.html [Accessed 03 July 2017]

[6] Weisstein, Eric W. *Lyapunov Characteristic Exponent*. From MathWorld–A Wolfram Web Resource. http://mathworld.wolfram.com/LyapunovCharacteristicExponent.html [Accessed 26 July 2017]

[7] Cross, Michael. *Physics 161: Introduction to Chaos - Chapter 7*. 2000. Available from: http://www.cmp.caltech.edu/~mcc/Chaos_Course/ [Accessed 28 July 2017]

[8] Sprott, Julien. *Numerical Calculation of Largest Lyapunov Exponent*. Available from: http://sprott.physics.wisc.edu/chaos/lyapexp.htm [Accessed 26 July 2017]

[9] Gottwald, George and Melbourne, Ian.*On the Implementation of the 0–1 Test for Chaos*. Available from: https://arxiv.org/pdf/0906.1418.pdf [Accessed 21 August 2017]

[10] Grassberger, Peter and Procaccia, Imatar. Measuring the strangeness of strange attractors, *Physica D, Nonlinear phenomena*, 1983. Volume 9, (issues 1-2). Available from: http://www.sciencedirect.com/science/article/pii/0167278983902981 [Accessed 15 August 2017]

[11] Ott, Edward. *Attractor dimensions*, Available from: http://www.scholarpedia.org/article/Attractor_dimensions. [Accessed 29 August 2017]